



RESEARCH LETTER

10.1002/2016GL068607

Key Points:

- The slow solar wind is formed via magnetic reconnection along the S-Web
- Periodic density structures are formed in the solar atmosphere
- High-resolution composition data constrain models of slow solar wind formation and release

Correspondence to:

L. Kepko,
larry.kepko@nasa.gov

Citation:

Kepko, L., N. M. Viall, S. K. Antiochos, S. T. Lepri, J. C. Kasper, and M. Weberg (2016), Implications of L1 observations for slow solar wind formation by solar reconnection, *Geophys. Res. Lett.*, *43*, 4089–4097, doi:10.1002/2016GL068607.

Received 9 MAR 2016

Accepted 18 APR 2016

Accepted article online 22 APR 2016

Published online 5 MAY 2016

Implications of L1 observations for slow solar wind formation by solar reconnection

L. Kepko¹, N. M. Viall¹, S. K. Antiochos¹, S. T. Lepri², J. C. Kasper², and M. Weberg²

¹NASA Goddard Space Flight Center, Greenbelt, Maryland, USA, ²Department of Climate and Space Science and Engineering, University of Michigan, Ann Arbor, Michigan, USA

Abstract While the source of the fast solar wind is known to be coronal holes, the source of the slow solar wind has remained a mystery. Long time scale trends in the composition and charge states show strong correlations between solar wind velocity and plasma parameters, yet these correlations have proved ineffective in determining the slow wind source. We take advantage of new high time resolution (12 min) measurements of solar wind composition and charge state abundances at L1 and previously identified 90 min quasiperiodic structures to probe the fundamental timescales of slow wind variability. The combination of new high temporal resolution composition measurements and the clearly identified boundaries of the periodic structures allows us to utilize these distinct solar wind parcels as tracers of slow wind origin and acceleration. We find that each 90 min (2000 Mm) parcel of slow wind has near-constant speed yet exhibits repeatable, systematic charge state and composition variations that span the entire range of statistically determined slow solar wind values. The classic composition-velocity correlations do not hold on short, approximately hourlong, time scales. Furthermore, the data demonstrate that these structures were created by magnetic reconnection. Our results impose severe new constraints on slow solar wind origin and provide new, compelling evidence that the slow wind results from the sporadic release of closed field plasma via magnetic reconnection at the boundary between open and closed flux in the Sun's atmosphere.

1. Introduction

The solar wind has historically been divided into “fast” (>500 km/s) and “slow” (<500 km/s) components, based on the bulk speed of the ambient plasma. The fast solar wind is known to emanate from the interiors of coronal holes, but there is active debate over whether the slow wind originates from open field lines at the edge of the coronal holes or from closed field lines somewhere within the closed field, streamer belt, regions [Antiochos *et al.*, 2011; Zhao and Fisk, 2011; Wang *et al.*, 2012]. A distinguishing characteristic of the slow solar wind is the high variability of the plasma parameters, such as magnetic field, velocity, density, composition, and charge state [Buergi and Geiss, 1986; McComas *et al.*, 1998a; Zurbuchen *et al.*, 1998; Zurbuchen, 2002; Fisk *et al.*, 2003; Gloeckler *et al.*, 2003]. Due to the observed rigid rotation of coronal holes, magnetic reconnection between open and closed magnetic fields (known as interchange reconnection) must be occurring at the boundary of coronal holes [Wang *et al.*, 1988; Nash *et al.*, 1988; Wang and Sheeley, 1993; Lionello *et al.*, 2005], and there is substantial evidence of in situ variability created by interchange reconnection [Crooker *et al.*, 1996; Zurbuchen *et al.*, 1998; Zhao and Fisk, 2011; Owens *et al.*, 2013]. Yet a full understanding of the slow wind source has remained elusive.

Understanding either type of wind requires knowledge of both the source of the plasma (i.e., magnetically open coronal holes or closed streamer belts) and the process that accelerates this plasma to supersonic speeds. Important clues to the origin and acceleration of the solar wind are contained in the observed relationships between solar wind velocity and charge state and composition. Solar wind charge state ratios (e.g., O⁷⁺/O⁶⁺ and C⁶⁺/C⁵⁺), which are a proxy for the electron temperature, T_e , in the solar corona, and solar wind elemental composition abundances, related to processes in the source region, are believed to be set before or early in the solar wind release and acceleration process. As the corona expands and collision rates drop, these properties are then “frozen in” to the solar wind plasma and, unlike the solar wind velocity, do not evolve as the solar wind advects to 1 AU [Zhao and Fisk, 2011]. Solar wind composition measurements at

©2016. The Authors.

This is an open access article under the terms of the Creative Commons Attribution-NonCommercial-NoDerivs License, which permits use and distribution in any medium, provided the original work is properly cited, the use is non-commercial and no modifications or adaptations are made.

1 AU therefore maintain imprints of the conditions under which the solar wind formed, and as a result these properties can be used as tracers of solar wind source and acceleration. For example, several studies have demonstrated that the $A_{\text{He}} = \text{He}/\text{H}$ abundance ratio is not only proportional to the solar wind speed [e.g., *Ogilvie and Burlaga, 1974; Aellig et al., 2001*] but remarkably linear up to ~ 550 km/s, especially during solar minimum [*Kasper et al., 2007*]. The 12 h Ulysses Solar Wind Ion Composition Spectrometer (SWICS) composition data have revealed that the $\text{O}^{7+}/\text{O}^{6+}$ ratio is also well correlated with the measured solar wind speed [*Gloeckler et al., 2003*], while a similar relationship is found using the $\text{C}^{6+}/\text{C}^{5+}$ charge state ratio [*von Steiger, 2008*]. In fact, since stream interactions can modify the speed as the wind expands far from the Sun, obscuring the original speed after acceleration, such studies have concluded that charge state ratios and elemental abundance ratios can be used to determine solar wind source and acceleration much more precisely than the wind speed itself.

These robust statistical results of long-term variability have been used successfully to constrain theories of fast solar wind origin and acceleration. As demonstrated definitively by Ulysses [*McComas et al., 2008*], there is clear evidence that the fast wind source at the Sun is the open flux of long-lived (>1 day) coronal holes. The acceleration mechanism, however, is still not understood in detail. Two general mechanisms have been proposed for heating and acceleration in coronal holes: wave/turbulence [*Cranmer et al., 2007; Velli, 1993; Hollweg and Isenberg, 2002*] and interchange reconnection between open fields and small closed flux regions embedded within the hole [e.g., *Parker, 1992; Axford and McKenzie, 1992*]. Note that even with the reconnection mechanism, waves play a central role, because most of the energy released is believed to propagate away from the reconnecting site in the form of Alfvén waves [*Fisk, 2003*]. Although many important questions are still unanswered, a broad consensus has developed on the general features of fast wind origin and acceleration.

The origin of the variable slow wind, on the other hand, is far from understood, although several clear trends are recognized. Observations strongly suggest that its source at the Sun is somehow associated with the coronal closed field regions known as the streamer belts. The heliospheric current sheet (HCS), which maps down to the streamer belt boundary at the Sun and marks the polarity interface between inward and outward magnetic field, is always embedded in the slow wind, never the fast [*Burlaga and Ness, 2012*]. Furthermore, the average elemental abundances of the slow wind are similar to the abundances of the closed field corona, which are clearly different than the abundances of the photosphere or of the fast wind [*Geiss et al., 1995a*]. Finally, the inferred freeze-in temperature of the slow wind source is substantially higher than that of the fast wind and is more compatible with the higher temperatures of the closed corona than of coronal holes [*Geiss et al., 1995a*].

Given these associations, three general models have been proposed for the slow wind origin: *expansion factor*, *interchange*, and *S-Web*. The *expansion factor model* postulates that the slow wind origin is physically identical to the fast wind, except that the heating and acceleration occur on open flux tubes near the open-closed boundary, rather than in the coronal hole [*Withbroe, 1988; Wang et al., 1996*]. Boundary flux tubes generally expand much faster than flux tubes in the central regions of a coronal hole, undergoing so-called superradial expansion. Under this condition, even a steady Alfvén wave flux input can result in a solar wind that is slow and has charge states substantially different than in flux tubes with radial expansion [*Cranmer et al., 2007*]. Although this has yet to be demonstrated quantitatively, the long-term average elemental abundances of the slow wind may also be explained by the effects of flux tube geometry [*Cranmer et al., 2007*].

The *interchange model*, which operates on closed flux tubes, is in many ways the complete opposite of the expansion factor model. This model postulates that the slow wind source is within the closed corona. Open flux diffuses throughout the seemingly closed field region as a result of continuous interchange reconnection, which also results in the release of closed field plasma into the heliosphere [*Fisk et al., 1998; Schwadron et al., 1999*]. This model naturally explains the difference in abundances and charge state between fast and slow wind, because the properties of the resultant wind are proportional to loop length: smaller and cooler loops lead to fast wind, while larger, hotter loops lead to slow wind [*Zurbuchen et al., 1998; Fisk, 2003*]. Furthermore, the model is inherently dynamic, which can account for the observed slow wind variability, and the interchange reconnection that is the defining feature of the model may play an important role in heating and accelerating the plasma after it has been released onto open field lines [*Fisk et al., 2003; Fisk, 2003*]. It remains to be demonstrated, however, that the postulated open field diffusion actually occurs on the real Sun [*Edmondson et al., 2010*].

The *S-Web model* [Antiochos *et al.*, 2011], which is based on the classic streamer top models [Suess *et al.*, 1996; Endeve *et al.*, 2004; Rappazzo *et al.*, 2005], can be thought of as intermediate to the other two. This model is also inherently dynamic and invokes the release of closed field plasma onto open field lines, but only in a limited region about the open-closed boundary. The underlying hypothesis is that the open-closed boundary is dynamic, with closed flux opening up and open flux closing down as a result of instabilities or direct driving by the photosphere [Antiochos *et al.*, 2011]. In addition to field line opening and closing, there is likely to be continuous interchange reconnection between the open and closed field lines. An essential feature of the model is that as a result of the observed distributions of magnetic flux at the photosphere, the open-closed boundary in the corona must have extreme complexity, which results in the release of closed plasma over a dense web of separatrixes and quasi separatrixes in the heliosphere, the so-called *S-Web* [Antiochos *et al.*, 2011]. The topological complexity of the *S-Web* is essential in order to reconcile the model with the observations that slow wind often has large angular extent [Crooker *et al.*, 2004]. The acceleration process for the wind is similar to that of the interchange model in that it is due to the energy released by reconnection. A key difference between the two models, however, is that in the *S-Web* the reconnection can occur between closed flux resulting in the release of a plasmoids into the heliosphere, or between open flux, resulting in the generation of disconnected flux [Crooker *et al.*, 2002].

Although the three models above invoke different origins for the slow wind, the observations to date have proven to be inadequate for determining the validity of these models. All three models can readily account for the slowness of the wind, and the location of the source region is not as easily testable as the association between distinct coronal holes and fast wind. In part, this is also due to the complex magnetic topology of the streamer belt and closed field lines compared to coronal hole field lines. While the models all invoke a source region near the open-closed boundary, tracing plasma measured in situ at 1 AU back to the corona inevitably contains large uncertainties, especially in regions where coronal currents create departures from the predictions of simple force-free potential models [MacNeice *et al.*, 2011]. It appears, therefore, that the most effective tests of the models would be comparison with the charge state and elemental composition data. However, these have also proved inconclusive, in part because the comparisons have focused on the long time scale trends in these data, largely due to lack of counting statistics. These results average out much of the intrinsic dynamics of the slow wind source; consequently, the data cannot distinguish between quasi-steady models such as the expansion factor and fully dynamic ones such as the interchange or yield significant constraints as to the nature of the slow wind dynamics.

In order to make progress on identifying the source and acceleration mechanism of the slow wind, we must move beyond long-term averages and determine the fundamental time scales for the charge state and elemental composition variability. There is strong evidence of an ~ 90 min fundamental time scale using Sun Earth Connection Coronal and Heliospheric Investigation (SECCHI) and in situ plasma measurements [Viall *et al.*, 2009a; Viall and Vourlidas, 2015], but these studies have lacked the needed elemental composition data to make definitive conclusions. We take advantage of a new data set of high time resolution (12 min) measurements of the charge state abundances recently produced by the ACE SWICS science team for specified intervals [Shearer *et al.*, 2014]. We use these new data to study an interval of slow solar wind containing quasiperiodic structures in the number density. These periodic density structures (PDSs) were previously studied from a perspective of magnetospheric oscillations [Kepko and Spence, 2003], but now we focus on the high-resolution elemental composition properties of the wind. The combination of high temporal resolution composition measurements and the clearly identified boundaries of the periodic structures allow us to probe the elemental structure and dynamics of the slow solar wind. We show below that our results at this comparatively high time resolution place new and critical constraints on the possible source and acceleration mechanism for the slow wind. In particular, the data argue strongly for magnetic reconnection as the underlying process driving the dynamics.

2. Plasma Variability

The periodic density structures under study were observed from ~ 11 to 22 UT on 15 June 1999, by both the ACE and Wind spacecraft, located near L1 at (231, 34, and -14) and (205, -21 , and -8) R_E (Earth radius) GSE (geocentric solar ecliptic), respectively. Plasma and composition data from ACE Solar Wind Electron, Proton, and Alpha Monitor (SWEPAM) [McComas *et al.*, 1998b] and Solar Wind Ion Composition Spectrometer (SWICS) [Gloeckler *et al.*, 1998] and Wind 3DP [Lin *et al.*, 1995] and Solar Wind Experiment (SWE) [Ogilvie *et al.*, 1995] are shown in Figure 1. The proton (Figure 1d) and He (Figure 1e) number density measurements from

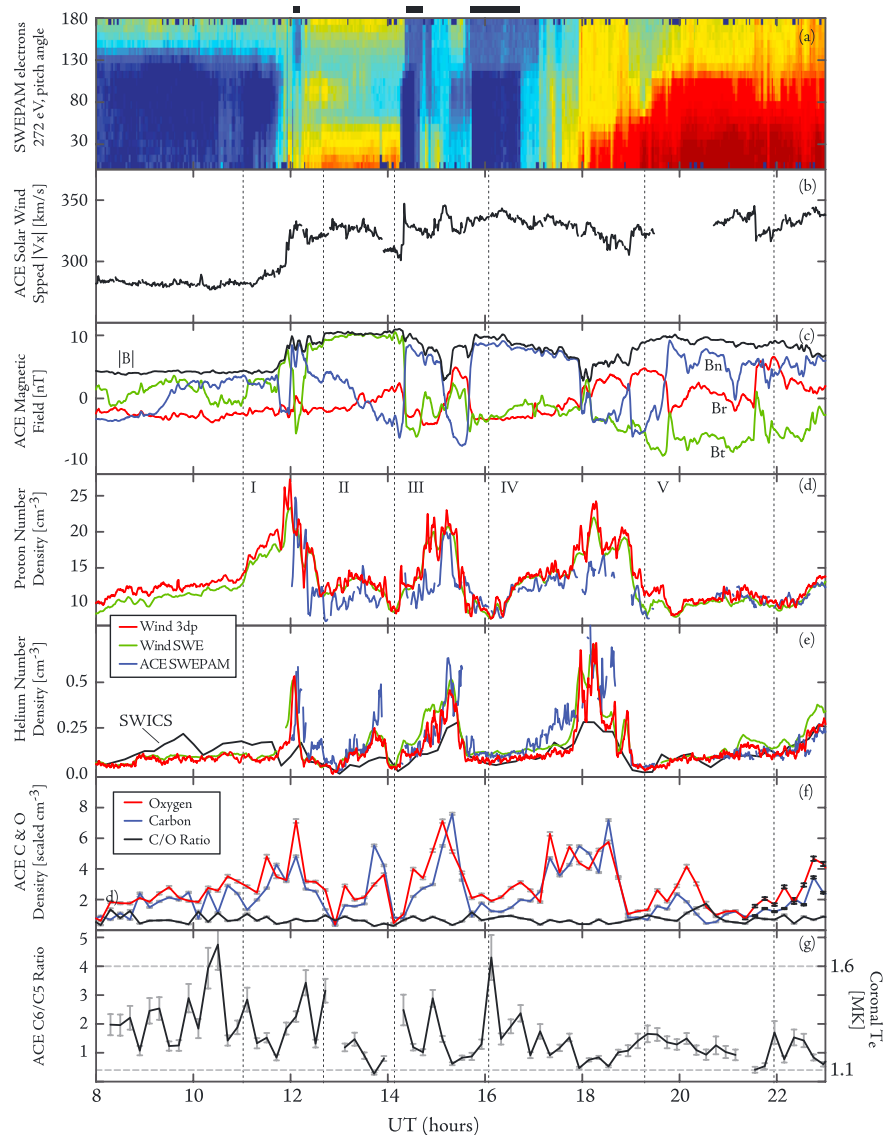


Figure 1. In situ observations of the periodic density structures (labeled I–V) observed by the ACE and Wind spacecraft near 1 AU on 15 June 1999. Plotted are (a) 272 eV electron pitch angles from ACE SWEPAM; (b) ACE solar wind velocity, $|V_x|$; (c) ACE magnetic field observations in RTN coordinates; (d) proton number density from ACE and Wind; (e) helium number density from ACE and Wind; (f) oxygen ($\times 1 \times 10^{-3}$) and carbon ($\times 2 \times 10^{-3}$) number densities and C/O ratio; (g) the C^{6+}/C^{5+} ratio measured by ACE SWICS. Ratio values of 4 are equivalent to 100% C^{6+} , within the resolution of the measurements. Error bars shown for ACE SWICS data in Figures 1f and 1g represent the statistical uncertainty and are on average less than 10% for the abundances and $\sim 30\%$ for the charge state ratio. Data with relative errors greater than 50% have been neglected in the analysis. Horizontal lines show inferred coronal temperature T_e . Black bars at the top of the figure indicate times of magnetic disconnection from the Sun, as inferred by the electron heat flux data.

both spacecraft provide an overview of the characteristic features of the periodic structures and indicate the level of agreement between three independent plasma instruments on two spacecraft. Each ~ 90 min PDS is identified with the labels I–V, while the boundaries, corresponding to local minima of the large-scale (~ 90 min) solar wind number density structures, are marked with vertical lines. The solar wind proton number density increased for each density structure by up to a factor of ~ 3 , peaking in the midpoint of each structure then returned to the background level. The He data also exhibit repeated, cyclic, behavior on the same ~ 90 min time scale, rising approximately linearly at the start of each PDS then rapidly decrease to the background value in the latter half of the event. Note that the He peak and rapid decrease occur after the midpoint of each density structure. The data from both the Wind and ACE spacecraft exhibit strong similarity and confirm that these are azimuthally coherent structures at the separation scale of the spacecraft ($\sim 55 R_E$

= 350 Mm). As shown by *Kepko and Spence [2003]*, these PDSs directly drove magnetospheric pulsations ~ 1 h later, after connecting to Earth. These periodic structures are not waves or oscillations. Instead, they are recurrent enhancements in the number density, in quasi pressure balance with the magnetic field, entrained in the solar wind. The solar wind velocity remained relatively constant for each periodic density structure, with the exception of a 50 km/s increase in the middle of event I and a small jump at the boundary of PDS II and III (Figure 1b).

The carbon and oxygen elemental abundances and the C^{6+}/C^{5+} charge state ratios and associated errors measured by ACE SWICS are shown in Figures 1f and 1g, respectively, at 12 min resolution. While the C/O ratio remained relatively constant at ~ 0.7 , the C and O densities varied significantly, but in a repeatable manner. For all five PDSs the abundances show a consistent pattern of peaking in the middle of the structure, followed by a rapid decrease before the start of the next event, with minima occurring at the PDS boundaries. The C^{6+}/C^{5+} ratio for PDS IV, which occurred between 16 and 20 UT, shows a linear decrease during the 4 h of the event, from an effective T_e of 1.6 to 1.1 MK. Event V shows a similar slow decrease. The previous events II and III are suggestive of this behavior as well, although the data are noisy. Even though the C and O measurements are at lower time resolution than the proton and He measurements, and with larger variability, the fact that they track the higher resolution He measurements which were obtained from two independent spacecraft with three different instruments lends support to our claim that charge state and ion abundance also varied within these periodic structures.

3. Discussion

The periodic density structures shown in Figure 1 exhibited a repeatable signature in plasma composition that clearly distinguishes them from random variability. Each structure began as “normal” slow solar wind, with low speed and low He, C, and O abundances. The proton density then increased by up to a factor of 3, reaching the maximum near the midpoint of the structure. The He, C, and O abundances also rose during each event, generally peaking in the latter part of the structure. While the proton number density throughout the structure is consistent with values expected for the slow solar wind, the abundances of the heavier elements rose to values typically associated with the fast wind. For PDS II–V, the C^{6+}/C^{5+} charge state ratio begins with a high, slow wind value (corresponding to high coronal T_e) but ends with a lower, typically fast wind value (corresponding to low T_e). At the end of each PDS, the solar wind returns to a normal slow solar wind state to begin the cycle anew. These clearly defined, repeating compositional structures argue strongly for an imprinted coronal source rather than in-transit turbulence as the cause. The key point is that although the train of structures began with a modest jump (50 km/s) in velocity, the wind speed remained relatively constant at $\sim 320 \pm 20$ km/s throughout the entire event. While the slow solar wind density is known to be highly variable, it is the systematic, repeatable behavior of the solar wind plasma composition during this event, without a concomitant change in speed, which provides a critical new constraint on solar wind origin and acceleration.

3.1. Comparison to Previous Studies

As discussed in section 1, numerous studies have established definitive statistical correlations between solar wind composition and charge state and wind speed on long time scales. Our results, however, prove that these correlations do not hold on time scales less than a few hours. For example, *Kasper et al. [2007]* studied 27 day averages of V and the He/H ratio, A_{He} , during solar minimum and found a linear correlation,

$$A_{\text{He}}(V) = G(V - V_0), \quad (1)$$

where the constants $G = 1.63 \times 10^{-2}$ km/s and $V_0 = 259$ km/s were determined empirically. Figure 2a shows a comparison of the observed A_{He} for the event presented here with the statistical results of *Kasper et al. [2007]*. The He abundance ratio is color coded to each periodic density structure. Each structure exhibits the full range of helium abundance ratios observed in the ambient solar wind by *Kasper et al. [2007]*, but without a change in solar wind speed, and does so with a repeatable, systematic pattern. Following equation (1), the measured A_{He} ratios imply a range of solar wind velocities of ~ 300 –550 km/s, even though the solar wind speed was consistently slow at ~ 320 km/s. Note also that the position of the 11 h average of A_{He} and V , indicated with a black circle, is quite close to the 27 day average values and the empirical correlation given by equation (1), confirming that this is a typical parcel of solar wind, at least in an average sense, and consistent with the large-scale, empirical results. Critically, the variation is not random but varies systematically during each PDS.

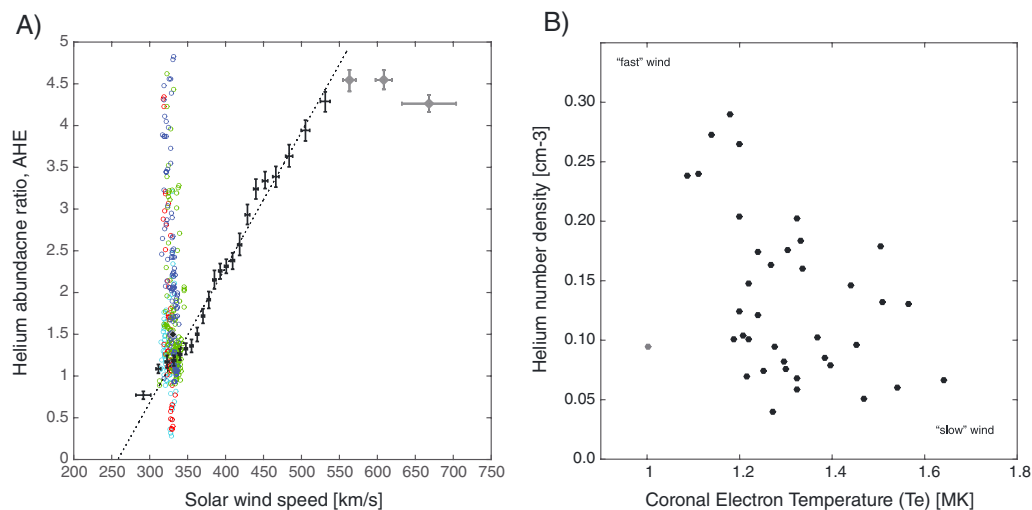


Figure 2. (a) Measurements of the A_{He} abundance ratios for this event plotted compared to the statistical result of *Kasper et al.* [2007]. A_{He} for each structure is color coded. The average of the observations is shown with a black diamond near $v = 330$ and $A_{He} = 1.5$ and lies very close to the empirical relationship, while the 12 min resolution data span the full range of measured values. The linear trend is for solar minimum conditions. Figure adapted from *Kasper et al.* [2007]. (b) The observed He density measured by ACE SWICS shows an inverse relationship with the inferred coronal electron temperature, T_e , calculated from the measured C^{6+}/C^{5+} charge state ratio, and spans a range that includes both fast and slow solar wind, despite the constant solar wind observed for this event. The grey data point at lower left was measured near the center of the flux rope of structure II.

A similar statistical correlation exists between the charge states of solar wind ions and wind speed. *Geiss et al.* [1995b], using daily averaged Ulysses SWICS data, demonstrated that the coronal temperature, T_e , determined from measured C^{6+}/C^{5+} ratios, varies inversely as a function of solar wind speed. Cooler coronal plasma (and higher A_{He}) is linked to higher solar wind speed, while hotter coronal plasma (and lower A_{He}) is linked to slower solar wind. The coronal temperatures inferred from the C^{6+}/C^{5+} ratios measured between 11 and 22 UT for the event presented here are plotted in Figure 2b versus the measured n_{He} . Compositionally fast wind resides in the upper left of the plot, while compositionally slow wind resides in the bottom right. Yet this full range of compositionally fast and slow wind occurred with little change in the solar wind velocity. We also note that extrapolating the *Geiss et al.* [1995b] relationship between T_e and solar wind velocity would imply a solar wind speed of ~ 350 – 600 km/s if the correlation held, similar to the velocity range predicted by the *Kasper et al.* [2007] formula.

It is important to note that the type of periodic 90 min structures presented here are not isolated phenomena but are ubiquitous features of the slow solar wind. In addition to numerous event studies [e.g., *Kepko et al.*, 2002; *Kepko and Spence*, 2003; *Villante et al.*, 2007], *Viall et al.* [2009b] showed through a thorough analysis of 11 years of solar wind data that periodic structures, ranging in size from 70 to 900 Mm (5 min to several hours in Earth's frame), are prevalent in the solar wind, occurring in up to 80% of slow solar wind intervals. Intriguingly, recent observations from STEREO HI1 and COR2 showed 90 min structures flowing away from the Sun beginning near 2.5 solar radii [*Viall and Vourlidas*, 2015], a compelling indicator of a solar source for these structures. *Viall et al.* [2009a] using in situ data demonstrated that He and protons were anticorrelated during a train of 30 min PDSs, also consistent with a solar source. Now with the high-resolution composition measurements presented here, particularly of C and O, and the C^{6+}/C^{5+} charge state ratios, we can rule out any in-transit development of these structures and demonstrate conclusively for the first time that the periodic density structures are formed in the solar atmosphere.

3.2. Magnetic Field Variability

In addition to the plasma variability, the magnetic variations during the periodic density structures provide critical constraints on their origin. The magnetic connectivity to the Sun can be determined by examining the field-aligned component of electrons, the so-called strahl, shown in Figure 1a. Elevated electron flux at angles of 0° (aligned with the magnetic field) and 180° (antialigned) indicate one end of the magnetic field line remains connected to the Sun, while flux at both angles indicate both ends of the field line are connected. A disappearance of this strahl is evidence of a magnetic disconnection event, where the local magnetic field is no

longer connected to the Sun. Evidence for all three types of connectivity are evident throughout the interval. Two clear disconnection events are indicated in Figure 1 (black bars at top), both located at the boundaries of the density structures, while a third, brief, disconnection occurred near the beginning of the PDS train.

Using these data, we can determine a qualitative picture of the magnetic topology of the entire interval. PDS II, from ~ 1245 to 1415 UT, shows clear signatures of a magnetic flux rope. The smooth rotation of the B_n component from positive to negative, the small radial component B_r , and a strong azimuthal field, B_t , with an increase in total field at the center of the interval, indicate a flux rope with an axis lying roughly in the ecliptic plane and perpendicular to the solar wind flow. The next structure, III, is bounded on either side by magnetic disconnection events indicated by heat flux drop out. Both before and after the structure, the magnetic field is entirely disconnected from the Sun. The switch in direction of the electron heat flux (in the middle of event IV near 15 UT) indicates the crossing of the heliospheric current sheet (HCS), to field lines that connect to opposite sides of the streamer back at the Sun. The disconnections and rapidly varying heat flux signatures, along with the discontinuous magnetic field jumps, are evidence of solar magnetic reconnection and a concomitant change in topology back in the corona as being responsible for the generation of these structures.

3.3. Implications for Slow Wind Models

The major conclusion from our study is that the slow solar wind exhibits a quasiperiodic variability with a time scale of ~ 90 min, with a repeatable, systematic, elemental abundance signature. Further, on this time scale, the wind speed shows no correlation with the repeatable charge state or elemental abundance signatures. This result has far-reaching implications for understanding slow wind origin. First, it rules out all quasi-steady models such as the expansion factor. In the quasi-steady models the solar wind plasma properties in any flux tube are set by the geometry of the flux tube in the corona, which determines the heating and momentum deposition along that flux tube. In such a model the charge state and velocity are inevitably tightly correlated: the heating determines the plasma pressure, which determines the velocity, and these together determine the charge states. The quasi-steady model, therefore, is excellent at reproducing the time-averaged correlations observed between velocity and composition, but our results show that on the fundamental time scale of the slow wind variability, the velocity, charge state, and composition are uncorrelated. We find a broad range of freeze-in temperatures and composition for the same wind velocity, in complete contradiction to what a quasi-steady model would predict. In principle, our observations are consistent with a constant solar wind whose properties are set by the expansion factor model, provided that magnetic reconnection adds transients to that solar wind. However, if the transients themselves form elemental building blocks of the slow solar wind, as we argue here, it obviates the need for an additional heating and release mechanism.

The lack of correlation between wind speed and charge state is also difficult to reconcile with the interchange model. Although this model is inherently dynamic, the interchange reconnection required for the open flux to diffuse throughout the closed field region must be so rapid that the evolution can be considered as statistically quasi-steady. In fact, this reasoning has been used to derive an inverse correlation between coronal temperature and wind speed V_{sw} , $V^2 \propto 1/T_e$ [Fisk *et al.*, 2003]. Since T_e is related directly to the charge state, this result implies that the velocity and charge state should be correlated, which again is contrary to what we observe.

The 90 min quasiperiodicity and the magnetic field variations that we observed for the slow wind structures provide further compelling evidence against the expansion factor and interchange models. It is evident from Figure 1 that magnetic variations are an integral feature of the slow wind structure. While magnetic topology changes are obviously counter to the expansion factor model, they also contradict the interchange model. This model would predict that the magnetic variability is due only to interchange reconnection, without evidence of the disconnections or biconnected flux ropes that are clearly present in our data. The topological variations that we observe are most easily understood as due to magnetic reconnection between open flux at the HCS, creating disconnections, and between expanding closed flux, creating biconnected flux ropes. The recent remote observations of quasiperiodic structures in streamer stalks close to the Sun [Viall and Vourlidas, 2015], as well as the tracking of streamer blobs out to 1 AU [Rouillard *et al.*, 2010a, 2010b], provide further evidence for this type of reconnection-driven evolution.

From the discussion above, we conclude that the slow wind is due to the periodic release of closed field plasma at the streamer boundary, and the elemental variability of the slow wind is best understood in terms of an S-Web type model. While our observations do not necessarily preclude wave heating of the solar wind or the expansion factor model for solar wind, they do show that magnetic reconnection is a fundamental part

of the release of slow solar wind plasma. Consequently, the S-Web is the most likely model for explaining all the features of this event, in particular, the presence of both disconnected flux and flux tubes connected at both ends back to the Sun. In the event shown in *Viall et al.* [2009a], the compositional signatures were such that the alphas were in antiphase, whereas here the alphas are shifted. This implies that the details of compositional changes and plasma release are likely to vary from event to event, as expected with the S-Web. Regardless of the details, during an interval of periodic density structures compositional changes exist that are consistent with formation back at the Sun. It is intriguing to note that a 90 min time scale at 1 AU corresponds roughly to a size scale of supergranule back at the Sun when accounting for expansion [Borovsky, 2008], so it may be that the observed quasiperiodic structures are due to the driving of the open-closed boundary by the quasi-regular supergranular convection. Our results provide compelling evidence that the slow wind is inherently dynamic and that the dynamics are not due to turbulence developing in situ but to some magnetically driven process occurring at the wind source. Our results, therefore, have laid the groundwork for a host of future observational studies and have set severe new constraints on any future modeling of the slow solar wind.

Acknowledgments

L.K. acknowledges the support of the NASA Guest Investigator Program, and S.K.A. acknowledges the support of the NASA Living With a Star Program. ACE and Wind plasma and magnetic field data were obtained from CDAWeb (<http://cdaweb.gsfc.nasa.gov>). The 12 min ACE SWICS composition data are available for the interval presented here by contacting the authors.

References

- Aellig, M. R., A. J. Lazarus, and J. T. Steinberg (2001), The solar wind helium abundance: Variation with wind speed and the solar cycle, *Geophys. Res. Lett.*, *28*(1), 2767–2770.
- Antiochos, S. K., Z. Mikic, V. S. Titov, R. Lionello, and J. A. Linker (2011), A model for the sources of the slow solar wind, *Astrophys. J.*, *731*(2), 112.
- Axford, W. I., and J. F. McKenzie (1992), The origin of high speed solar wind streams, in *Solar Wind Seven Colloquium*, edited by E. Marsch and R. Schwenn, pp. 1–5, Pergamon Press, Oxford, U. K.
- Borovsky, J. E. (2008), Flux tube texture of the solar wind: Strands of the magnetic carpet at 1 AU?, *J. Geophys. Res.*, *113*, A08110, doi:10.1029/2007JA012684.
- Buergi, A., and J. Geiss (1986), Helium and minor ions in the corona and solar wind—Dynamics and charge states, *Sol. Phys.*, *103*, 347–383.
- Burlaga, L. F., and N. F. Ness (2012), Magnetic field fluctuations observed in the heliosheath by Voyager 1 at 114 ± 2 AU during 2010, *J. Geophys. Res.*, *117*, A10107, doi:10.1029/2012JA017894.
- Cranmer, S. R., A. A. van Ballegoijen, and R. J. Edgar (2007), Self-consistent coronal heating and solar wind acceleration from anisotropic magnetohydrodynamic turbulence, *Astrophys. J. Suppl. Ser.*, *171*(2), 520–551.
- Crooker, N. U., M. E. Burton, J. L. Phillips, E. J. Smith, and A. Balogh (1996), Heliospheric plasma sheets as small-scale transients, *J. Geophys. Res.*, *101*(A), 2467–2474.
- Crooker, N. U., J. T. Gosling, and S. W. Kahler (2002), Reducing heliospheric magnetic flux from coronal mass ejections without disconnection, *J. Geophys. Res.*, *107*, 1028, doi:10.1029/2001JA000236.
- Crooker, N. U., C. L. Huang, S. M. Lamassa, D. E. Larson, S. W. Kahler, and H. E. Spence (2004), Heliospheric plasma sheets, *J. Geophys. Res.*, *109*, A03107, doi:10.1029/2003JA010170.
- Edmondson, J. K., S. K. Antiochos, C. R. DeVore, B. J. Lynch, and T. H. Zurbuchen (2010), Interchange reconnection and coronal hole dynamics, *Astrophys. J.*, *714*, 517–531, doi:10.1088/0004-637X/714/1/517.
- Endeve, E., T. E. Holzer, and E. Leer (2004), Helmet streamers gone unstable: Two-fluid magnetohydrodynamic models of the solar corona, *Astrophys. J.*, *603*, 307–321.
- Fisk, L. A. (2003), Acceleration of the solar wind as a result of the reconnection of open magnetic flux with coronal loops, *J. Geophys. Res.*, *108*(A4), 1157, doi:10.1029/2002JA009284.
- Fisk, L. A., N. A. Schwadron, and T. H. Zurbuchen (1998), On the slow solar wind, *Space Sci. Rev.*, *86*, 51–60, doi:10.1023/A:1005015527146.
- Fisk, L. A., G. Gloeckler, T. H. Zurbuchen, J. Geiss, and N. A. Schwadron (2003), Acceleration of the solar wind as a result of the reconnection of open magnetic flux with coronal loops, in *SOLAR WIND TEN: Proceedings of the Tenth International Solar Wind Conference. AIP Conference Proceedings*, pp. 287–292, Department of Atmospheric, Oceanic, and Space Sciences, Univ. of Michigan, Ann Arbor, Mich.
- Geiss, J., G. Gloeckler, and R. von Steiger (1995a), Origin of the solar wind from composition data, *Space Sci. Rev.*, *72*(1), 49–60.
- Geiss, J., et al. (1995b), The southern high-speed stream: Results from the SWICS instrument on Ulysses, *Science*, *268*(5), 1033–1036.
- Gloeckler, G., et al. (1998), Investigation of the composition of solar and interstellar matter using solar wind and pickup ion measurements with SWICS and SWIMS on the ACE spacecraft, *Space Sci. Rev.*, *86*(1), 497–539.
- Gloeckler, G., T. H. Zurbuchen, and J. Geiss (2003), Implications of the observed anticorrelation between solar wind speed and coronal electron temperature, *J. Geophys. Res.*, *108*(A4), 1158, doi:10.1029/2002JA009286.
- Hollweg, J. V., and P. A. Isenberg (2002), Generation of the fast solar wind: A review with emphasis on the resonant cyclotron interaction, *J. Geophys. Res.*, *107*, 1147, doi:10.1029/2001JA000270.
- Kasper, J. C., M. L. Stevens, A. J. Lazarus, J. T. Steinberg, and K. W. Ogilvie (2007), Solar wind helium abundance as a function of speed and heliographic latitude: Variation through a solar cycle, *Astrophys. J.*, *660*(1), 901–910.
- Kepko, L., and H. E. Spence (2003), Observations of discrete, global magnetospheric oscillations directly driven by solar wind density variations, *J. Geophys. Res.*, *108*(A), 1257, doi:10.1029/2002JA009676.
- Kepko, L., H. E. Spence, and H. J. Singer (2002), ULF waves in the solar wind as direct drivers of magnetospheric pulsations, *Geophys. Res. Lett.*, *29*(8), 1197–1200, doi:10.1029/2001GL014405.
- Lin, R. P., et al. (1995), A three-dimensional plasma and energetic particle investigation for the Wind spacecraft, *Space Sci. Rev.*, *71*(1), 125–153.
- Lionello, R., P. Riley, J. A. Linker, and Z. Mikic (2005), The effects of differential rotation on the magnetic structure of the solar corona: Magnetohydrodynamic simulations, *Astrophys. J.*, *625*(1), 463–473.
- MacNeice, P., B. Elliott, and A. Acebal (2011), Validation of community models: 3. Tracing field lines in heliospheric models, *Space Weather*, *9*, S10003, doi:10.1029/2011SW000665.
- McComas, D. J., et al. (1998a), Ulysses' return to the slow solar wind, *Geophys. Res. Lett.*, *25*(1), 1–4.

- McComas, D. J., S. J. Bame, P. Barker, W. C. Feldman, J. L. Phillips, P. Riley, and J. W. Griffee (1998b), Solar Wind Electron Proton Alpha Monitor (SWEPAM) for the advanced composition explorer, *Space Sci. Rev.*, *86*(1), 563–612.
- McComas, D. J., R. W. Ebert, H. A. Elliott, B. E. Goldstein, J. T. Gosling, N. A. Schwadron, and R. M. Skoug (2008), Weaker solar wind from the polar coronal holes and the whole Sun, *Geophys. Res. Lett.*, *35*, L18103, doi:10.1029/2008GL034896.
- Nash, A. G., N. R. J. Sheeley, and Y.-M. Wang (1988), Mechanisms for the rigid rotation of coronal holes, *Sol. Cycle Workshop*, *117*, 359–389.
- Ogilvie, K. W., and L. F. Burlaga (1974), A discussion of interplanetary postshock flows with two examples, *J. Geophys. Res.*, *79*(1), 2324–2330.
- Ogilvie, K. W., et al. (1995), SWE, a comprehensive plasma instrument for the wind spacecraft, *Space Sci. Rev.*, *71*(1), 55–77.
- Owens, M. J., N. U. Crooker, and M. Lockwood (2013), Solar origin of heliospheric magnetic field inversions: Evidence for coronal loop opening within pseudostreamers, *J. Geophys. Res. Space Physics*, *118*(5), 1868–1879.
- Parker, E. N. (1992), The X ray corona, the coronal hole, and the heliosphere, *J. Geophys. Res.*, *97*, 4311–4316, doi:10.1029/91JA01705.
- Rappazzo, A. F., M. Velli, G. Einaudi, and R. B. Dahlburg (2005), Diamagnetic and expansion effects on the observable properties of the slow solar wind in a coronal streamer, *Astrophys. J.*, *633*(1), 474–488.
- Rouillard, A. P., et al. (2010a), Intermittent release of transients in the slow solar wind: 1. Remote sensing observations, *J. Geophys. Res.*, *115*, A04103, doi:10.1029/2009JA014471.
- Rouillard, A. P., et al. (2010b), Intermittent release of transients in the slow solar wind: 2. In situ evidence, *J. Geophys. Res.*, *115*, A04104, doi:10.1029/2009JA014472.
- Schwadron, N. A., L. A. Fisk, and T. H. Zurbuchen (1999), Elemental fractionation in the slow solar wind, *Astrophys. J.*, *521*(2), 859–867.
- Shearer, P., R. von Steiger, J. M. Raines, S. T. Lepri, J. W. Thomas, J. A. Gilbert, E. Landi, and T. H. Zurbuchen (2014), The solar wind neon abundance observed with ACE/SWICS and Ulysses/SWICS, *Astrophys. J.*, *789*(1), 60.
- Suess, S. T., A. H. Wang, and S. T. Wu (1996), Volumetric heating in coronal streamers, *J. Geophys. Res.*, *101*(A9), 19,957–19,966.
- Velli, M. (1993), On the propagation of ideal, linear Alfvén waves in radially stratified stellar atmospheres and winds, *Astron. Astrophys.*, *270*, 304–314.
- Viall, N. M., and A. Vourlidas (2015), Periodic density structures and the origin of the slow solar wind, *Astrophys. J.*, *807*(2), 176.
- Viall, N. M., H. E. Spence, and J. Kasper (2009a), Are periodic solar wind number density structures formed in the solar corona?, *Geophys. Res. Lett.*, *36*, L23102, doi:10.1029/2009GL041191.
- Viall, N. M., L. Kepko, and H. E. Spence (2009b), Relative occurrence rates and connection of discrete frequency oscillations in the solar wind density and dayside magnetosphere, *J. Geophys. Res.*, *114*, A01201, doi:10.1029/2008JA013334.
- Villante, U., P. Francia, M. Vellante, P. Di Giuseppe, A. Nubile, and M. Piersanti (2007), Long-period oscillations at discrete frequencies: A comparative analysis of ground, magnetospheric, and interplanetary observations, *J. Geophys. Res.*, *112*, A04210, doi:10.1029/2006JA011896.
- von Steiger, R. (2008), The solar wind throughout the solar cycle, in *The Heliosphere Through the Solar Activity Cycle*, p. 41, Springer, Chichester, U. K.
- Wang, Y.-M., and N. R. J. Sheeley (1993), Understanding the rotation of coronal holes, *Astrophys. J.*, *414*, 916–927.
- Wang, Y.-M., N. R. J. Sheeley, A. G. Nash, and L. R. Shampine (1988), The quasi-rigid rotation of coronal magnetic fields, *Astrophys. J.*, *327*, 427–450.
- Wang, Y.-M., S. H. Hawley, and N. R. J. Sheeley (1996), The magnetic nature of coronal holes, *Science*, *271*(5), 464–469.
- Wang, Y.-M., R. Grappin, E. Robbrecht, and N. R. J. Sheeley (2012), On the nature of the solar wind from coronal pseudostreamers, *Astrophys. J.*, *749*(2), 182.
- Withbroe, G. L. (1988), The temperature structure, mass, and energy flow in the corona and inner solar wind, *Astrophys. J.*, *325*, 442–467, doi:10.1086/166015.
- Zhao, L., and L. Fisk (2011), Understanding the behavior of the heliospheric magnetic field and the solar wind during the unusual solar minimum between cycles 23 and 24, *Sol. Phys.*, *274*(1), 379–397.
- Zurbuchen, T. H. (2002), The solar wind composition throughout the solar cycle: A continuum of dynamic states, *Geophys. Res. Lett.*, *29*(9), 1352, doi:10.1029/2001GL013946.
- Zurbuchen, T. H., L. A. Fisk, G. Gloeckler, and N. A. Schwadron (1998), Element and isotopic fractionation in closed magnetic structures, *Space Sci. Rev.*, *85*(1), 397–406.